dimensional spherical neighbourhoods of the corresponding code words $\{S_i(L)\}$. Since the radia of these neighbourhoods are never greater than $\Delta N^{1/2}$, the following limit process holds:

$$(N, M, L) \to (N, M)_0 \quad \text{when } \Delta \to 0 \quad (L \to \infty) \qquad (3)$$

Results: A computer technique[10] is developed enabling the finding of the absolute minimum of function g. Using $f(x) = x^{-32}$, we obtain three groups of block codes, given in Table 1.

Table 1 SET OF (N, M, L) CODES OBTAINED BY MEANS OF COMPUTER

	Group 1	Group 2	Group 3
N	$R_N = \frac{1}{2}$ bit/dim	$R_N = \frac{2}{3}$ bit/dim	$R_N = 1$ bit/dim
3		(3, 4, 64)	(3, 8, 64)
4	(4, 4, 64)	(4, 6, 64)	(4, 16, 64)
5	(5, 6, 64)	(5, 10, 64)	(5, 32, 64)
6	(6, 8, 64)	(6, 16, 64)	(6, 64, 64)
7	(7, 12, 64)	(7, 25, 64)	
8	(8, 16, 64)	(8, 40, 64)	
9	(9, 22, 64)	(9, 64, 64)	
10	(10, 32, 64)		

In each column, the block codes are given according to the increasing dimensions and equal information rates R_N. The actual information rates of some codes are slightly different from those quoted above, because the integers M required by the above values of dimensions N to yield $R_N = \frac{1}{2}dM/N$ do not exist. In such cases, the integers M giving the information rates closest to the required rates are taken.

The efficiency chart[2,3] in Fig. 1 displays the difference between s.n.r. (in dB) needed to achieve a word error probability $P_e = 10^{-5}$ and SNR_{ideal} as a function of information rate R_N. SNR_{ideal} is determined from Shannon's capacity formula $SNR_{ideal} = 10 \log_{10} (2^{2R_N} - 1)$. The two solid curves labelled $N = 5$ and $N = 15$ are the lower bounds for optimal equal-energy block codes for the given values of dimensions.[2] It should be mentioned that, because of difficulty of calculating the exact word error probability of $\{(N, M, L)\}$ codes, its upper union bound is used.[9]

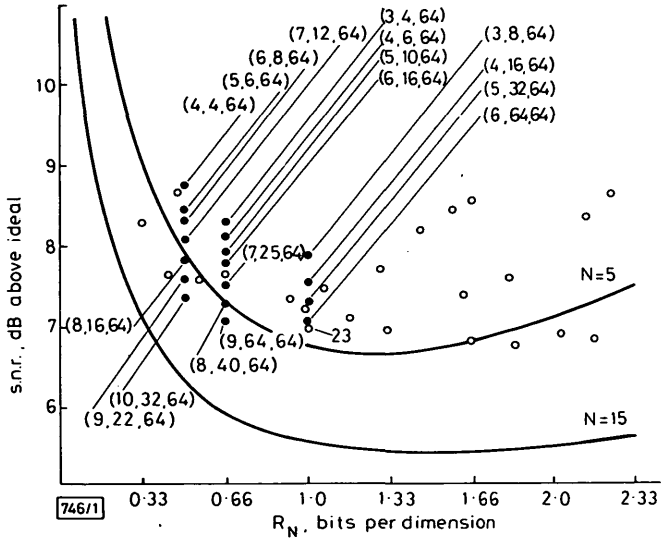

Fig. 1 *Performances of some $(N, M, 64)$ codes (denoted by ●) and permutation modulation codes[3] (denoted by ○) for word error probability $P_e = 10^{-5}$*

Conclusion: From Ziv's result, mentioned above, and from eqn. 3, it follows that the codes $\{(N, M, L)\}$ defined in this letter are asymptotically optimal only when $\Delta \to 0$ $(L \to \infty)$. However, even for finite values of L, these codes have good performances. Thus, for instance, the code (6, 64, 64) has almost the same properties as the permutation modulation code denoted by 23 in Fig. 1, whose dimension is 31 and whose number of code words is about $0{\cdot}2 \times 10^{10}$. However, the permutation modulation codes have a much smaller number of amplitude levels. From Fig. 1 we can conclude that, for all considered $\{(N, M, 64)\}$ codes, P_e decreases when N increases, R_N and the s.n.r. being constant. With further increase in N we hope to approach even closer to the Shannon bound for the values $L < 64$ also.

Acknowledgments: The author wishes to thank G. Lukatela and D. Drajić of the Faculty of Electrical Engineering, University of Belgrade, for their continued encouragement of the research and useful suggestions that led to this letter.

D. E. LAZIĆ

Faculty of Technical Sciences
University of Novi Sad
Institute of Measurement and Control
21000 Novi Sad, V. Vlahovića 3, Yugoslavia

17th December 1979

References

1 SHANNON, C. E.: 'Probability of error for optimal codes in a Gaussian channel', *Bell Syst. Tech. J.*, 1959, **38**, pp. 611–707
2 SLEPIAN, D.: 'Bounds on communication', *ibid.*, 1963, **42**, pp. 681–707
3 SLEPIAN, D.: 'Permutation modulation', *Proc. IEEE*, 1965, **53**, pp. 228–236
4 ZIV, J.: 'Generation of optimal codes by a "pyramid-packing" argument', *IEEE Trans.*, 1964, **IT-10**, pp. 253–255
5 LANDAU, J. H.: 'How does a porcupine separate its quills?' *IEEE Trans.*, 1971, **IT-17**, pp. 157–161
6 GILBERT, E. N.: 'A comparison of signaling alphabets', *Bell Syst. Tech. J.*, 1952, **31**, pp. 504–522
7 RICE, S. O.: 'Communication in the presence of noise—probability of error for two encoding schemes', *ibid.*, 1950, **29**, pp. 60–93
8 TOTH, F. L.: 'Lagerungen in der Ebene auf der Kugel und im Raum' (Springer-Verlag, Berlin, 1953), chap. 6
9 WOZENCRAFT, J. M., and JAKOBS, I. M.: 'Principles of communication engineering' (Wiley, New York, 1965), chap. 4, pp. 211–266
10 LAZIĆ, E. D.: 'On a class of codes approaching the Shannon bound'. MSc. thesis, Faculty of Electrical Engineering, University of Belgrade, 1979, pp. 43–77

0013-5194/80/050185-02$1.50/0

PHASE CORRECTION IN TWO-INTEGRATOR LOOP FILTERS USING NEW VARIABLE-PHASE INVERTING AMPLIFIER

Indexing terms: Circuit design, Filters

A novel variable-phase inverting amplifier is given. The proposed inverter has an adjustable phase which depends on the unity-gain bandwidth of only one of the two o.a.s employed in the circuit. Application of the inverter for phase correction in two-integrator loop filters is discussed.

One of the most popular dual-integrator loop filters is the Tow-Thomas biquad circuit[1–2] in which all the operational amplifiers (o.a.s) are used in a single-ended configuration. Although the circuit has very low passive sensitivities, it suffers from a rather drastic Q-factor enhancement. The Q-factor enhancement is due to the parasitic phase shift around the loop which is cumulative and lagging. Several passive[2–3] and active[4–7] compensation methods for phase correction have been reported. The method given in Reference 7 is based on replacing the unity-gain inverter of the biquad by a suitable phase lead inverter. The variable-phase inverter introduced by Reddy[7] has the advantage that the phase depends on the gain-bandwidth product of only one of the two o.a.s employed in the circuit.

The purpose of this letter is to introduce another variable-phase inverting amplifier having the same attractive feature as that in the Reddy inverter.[7] Besides it uses one resistor less than Reddy's inverter[7] (when employed in the Tow-Thomas biquad).

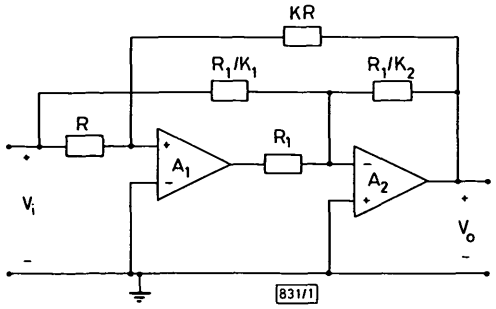

Fig. 1 *Novel variable-phase inverting amplifier*

Fig. 1 represents the new variable-phase inverting amplifier which employes two o.a.s in a single-ended configuration and five resistors. By direct analysis of the network, its transfer function is given by

$$\frac{V_0}{V_i} = -K\left\{1 + \left[\frac{K_1(K+1)}{K}\right]\frac{1}{A_1}\right\}\Big/\Big\{1 + [K_2(K+1)]\frac{1}{A_1} + [(K+1)(K_1+K_2+1)]\frac{1}{A_1A_2}\Big\} \quad (1)$$

Assume that each o.a. is characterised by a single-pole model with a unity-gain bandwidth ω_t. Thus the open-loop gain A of the o.a. is given by:

$$A_i(s) \approx \frac{\omega_{ti}}{s} \qquad (i = 1, 2) \quad (2)$$

For frequencies such that:

$$\omega \ll \omega_{t1}\left[\frac{K}{K_1(K+1)}\right] \qquad \omega \ll \omega_{t1}\left[\frac{1}{K_2(K+1)}\right]$$
$$\omega^2 \ll \omega_{t1}\omega_{t2}\left[\frac{1}{(K+1)(K_1+K_2+1)}\right] \quad (3)$$

Eqn. 1 reduces to:

$$\frac{V_0}{V_i} \approx -K\Big/\left[\frac{\omega}{\omega_{t1}}\right](K+1)\left(\frac{K_1}{K} - K_2\right) \quad (4)$$

Thus it is seen that in the frequency range given by eqn. 3, the network of Fig. 1 realises an inverting amplifier having a constant d.c. gain $= -K$, and a variable phase. The phase can be made leading, resulting in a phase-lead inverter which is suitable for phase correction in the two-integrator loop filters.

As an example, consider the well known Tow-Thomas biquad filter section,[1-2] which is unsuitable for high-Q high-frequency applications because of the undesired extra phase shift around the loop which is cumulative and lagging. Phase correction in this biquad can be achieved if its unity-gain inverter is replaced by the proposed amplifier resulting in the modified Tow-Thomas biquad filter section shown in Fig. 2. For simplicity of analysis, assume that matched o.a.s are used in the biquad section. Since the total phase lag at ω_0 resulting from the two integrators equals $(-2\omega_0/\omega_t)$, where ω_0 is the biquad pole radian frequency ($\omega_0 = 1/CR$), the inverter must be adjusted to provide a phase lead at ω_0 equal to $(2\omega_0/\omega_t)$. From eqn. 4 and for $K = 1$, the condition for phase correction around the loop is given by:

$$K_1 = K_2 + 1 \quad (5)$$

In this case the inverter transfer function simplifies to:

$$\frac{V_0}{V_i} = -\frac{1 + 2(K_2+1)\left(\frac{s}{\omega_t}\right)}{1 + 2K_2\left(\frac{s}{\omega_t}\right) + 4(K_2+1)\left(\frac{s}{\omega_t}\right)^2} \quad (6)$$

Thus the pole Q and the pole radian frequency of the inverter transfer function (when adjusted for phase correction in the Tow-Thomas biquad) are given by:

$$\omega_a = \frac{\omega_t}{2\sqrt{(K_2+1)}} \quad (7)$$

$$Q_a = \frac{\sqrt{(K_2+1)}}{K_2} \quad (8)$$

A figure of merit for the inverter is the $\omega_a Q_a$ product. For the proposed inverter $\omega_a Q_a = \omega_t/2K_2$. For a large figure of merit, it is clear that a small value of K_2 is desirable. From the stability point of view, however, there is a lower limit on the value of K_2 that can be used. The stability analysis is considered next.

Taking the second o.a. pole into account and assuming that it occurs at a frequency $\omega_2(\omega_2 > \omega_t)$, the open-loop gain A can be expressed as:[8]

$$A(s) \approx \frac{\omega_t}{s\left(1 + \frac{s}{\omega_2}\right)} \quad (9)$$

Substituting from eqns. 5 and 9 into eqn. 1, and after routine stability analysis, it follows that for a stable operation of the phase-lead inverter it is necessary that:

$$\frac{\omega_2}{\omega_t} > \left[\frac{1}{K_2} - \frac{K_2}{4(K_2+1)}\right] \quad (10)$$

For a given o.a. the design value for K_2 is determined from the above equation. Taking $K_2 = 1$, however, will ensure the inverter stability. In this case the figure of merit $= 0{\cdot}5\omega_t$. On the other hand, taking $K_2 = 0{\cdot}65$ results in a figure of merit $= 0{\cdot}77\omega_t$. In this case, however, the o.a. employed must have $\omega_2 > 1{\cdot}44\omega_t$.

In conclusion, a novel two-o.a.s plus five-resistor variable-phase inverting amplifier is given. The proposed inverter has an adjustable phase which depends on the unity-gain bandwidth of only one of the two o.a.s. Application of the inverter for phase correction in the Tow-Thomas biquad filter section is discussed. In this respect the modified biquad uses one resistor less than that in Reference 7 and employs the four o.a.s in a single-ended configuration. It is worth noting that the proposed amplifier may also be adjusted for phase compensation by taking $K_1 = KK_2$ (even if mismatched o.a.s are used). In this case, however, the amplifier will have no advantage over that in Reference 7.

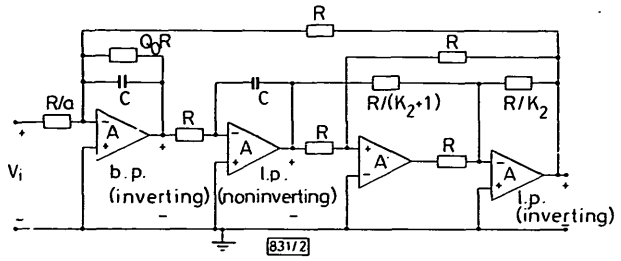

Fig. 2 *Improved Tow-Thomas biquad filter suitable for high Q and high frequency. Magnitude of gain at ω_0 at each of three outputs $= aQ_0$*

AHMED M. SOLIMAN
Department of Electrical Engineering
Florida Atlantic University
Boca Raton, Florida 33431, USA

22nd January 1980

References

1 TOW, J.: 'Active-*RC* filters—a state space realization', *Proc. IEEE*, 1968, **56**, pp. 1137-1139

2 THOMAS, L. C.: 'The biquad: Part I—some practical design considerations. Part II—a multipurpose active filtering system', *IEEE Trans.*, 1971, **CT-18**, pp. 350–361
3 SOLIMAN, A. M., and ISMAIL, M.: 'Phase correction in two-integrator loop filters using a single compensating resistor', *Electron. Lett.*, 1978, **14**, pp. 375–376
4 VOGEL, P. W.: 'Method for phase correction in active *RC* circuits using two integrators', *ibid.*, 1971, **7**, pp. 273–275
5 AKERBERG, D., and MOSSBERG, K.: 'A versatile active *RC* building block with inherent compansion for the finite bandwidth of the amplifier', *IEEE Trans.*, 1974, **CAS-21**, pp. 75–78
6 BRACKETT, P. O., and SEDRA, A. S.: 'Active compensation for high-frequency effects in op-amp circuits with applications to active filters', *ibid.*, 1976, **CAS-23**, pp. 68–72
7 REDDY, M. A.: 'Operational amplifier circuits with variable phase shift and their application to high-*Q* active-*RC* filters and *RC*-oscillators', *ibid.*, 1976, **CAS-23**, pp. 384–389
8 MARTIN, K., and SEDRA, A. S.: 'On the stability of the phase lead integrator', *ibid.*, 1977, **CAS-24**, pp. 321–324

0013-5194/80/050186-03$1.50/0

PULSE BROADENING IN LONG-SPAN DISPERSION-FREE SINGLE-MODE FIBRES AT 1·5 μm

Indexing terms: Optical fibres

Dispersion-free single-mode fibres at 1·5 μm were fabricated by controlling their waveguide dispersion and dopant-dependent material dispersion. Pulse broadening in the 20 km long fibre was measured by using a laser diode operated at 1·5 μm. Measured pulse broadening was 1·3 ps/km nm, which is in good agreement with theoretical results. The present experiment confirms that it is beneficial to use such fibres for large-capacity and long-distance transmission media.

Introduction: It has been shown experimentally and theoretically that the minimum loss in silica-based optical fibres is achieved around 1·5 μm.[1,2] In a conventional single-mode-fibre design, however, the bandwidth at this wavelength is no more than 60 MHz, owing to chromatic dispersion, when the fibre length is 100 km and the source bandwidth is 5 nm.[3] Several authors have reported that the zero-dispersion wavelength can be shifted towards the 1·5 μm wavelength region by choosing a suitable waveguide structure so as to cancel the material dispersion.[4–10] Such single-mode fibres in the 1·5 μm low-loss wavelength region are of great interest for long-distance and high-capacity transmission media.

In this letter, we describe the fabrication of dispersion-free low-loss single-mode fibres in the 1·5 μm region and pulse-broadening measurements in long-span zero-dispersion single-mode fibres.

Experiment: The single-mode fibres with GeO_2-doped silica core and pure silica cladding were prepared by the conventional m.c.v.d. method. The fibre parameters were chosen so as to shift the zero-dispersion wavelength towards the 1·5 μm wavelength region. The bending loss and splice loss were also taken into consideration when the fibre parameters were chosen.[6]

The refractive-index profiles and cutoff wavelength λ_c were measured by an interference microscope and the near-field pattern technique,[11] respectively. The dispersion of each fibre was measured by the difference method, using an optical parametric oscillator.[12]

The laser which was used for measuring the pulse broadening was of the InGaAsP/InP double-heterostructure type; the output at 1·5 μm was coupled into single-mode fibres by a microscopic lens.

The optical wave shape was observed with a Ge avalanche photodiode with a sensitive-area diameter of 100 μm.

Results and discussion: The relative refractive-index difference Δ between core and cladding must be higher than 0·5% to cancel the material dispersion and the waveguide dispersion, and to avoid high bending loss. On the other hand, higher relative refractive-index difference causes high splice loss, owing to small core diameters and excess loss due to waveguide imperfection. The relative refractive index difference of the fibres was designed to be between 0·5% and 0·6%, by taking into consideration the above conditions.

The fibre parameters used in this study are summarised in Table 1. The measured total losses of the 20 km long fibre, including the three splice losses, were 24·2 dB, 21 dB and 26·3 dB at 1·50 μm, 1·52 μm and 1·29 μm, respectively. The measured zero-dispersion wavelength, and the calculated value obtained from the refractive-index profiles measured with the

Table 1 FIBRE PARAMETERS

Fibre	A	B	C	D
Length, km	4·7	5·6	6·4	3·3
Outer diameter, μm	125	125	125	125
Δ, %	0·58	0·54	0·51	0·58
λ_c, μm	1·01	0·92	0·82	0·89
Core diameter*, μm	4·8	4·5	4·1	4·2
λ_0, calculated, μm	1·45	1·48	1·50	1·51
λ_0, observed, μm	1·46	1·50	1·50	1·46
Loss**, dB/km	0·8	1·02	1·14	0·91

* estimated from preforms
** at 1·52 μm

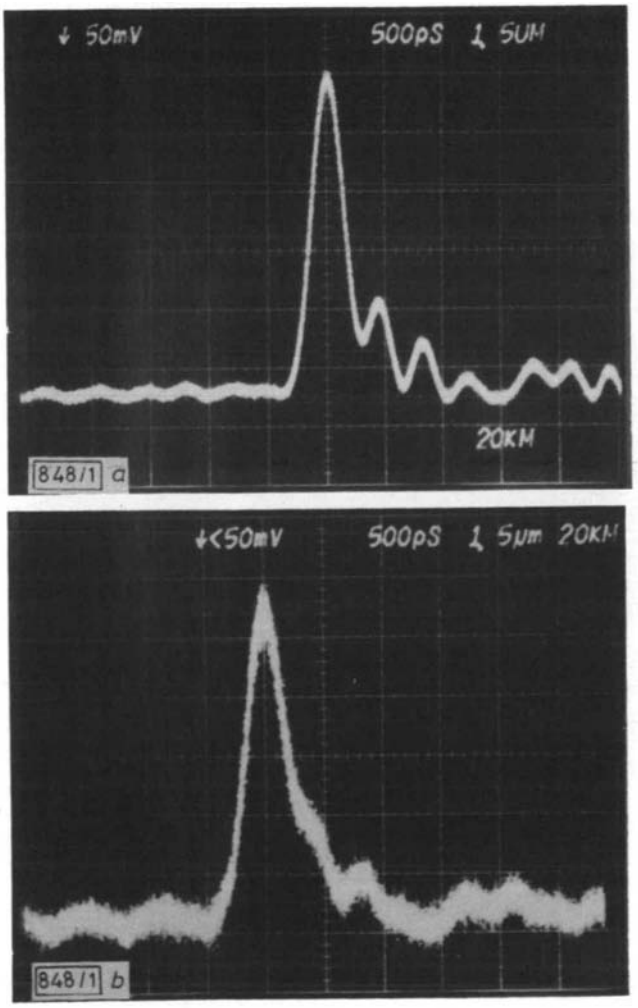

Fig. 1 *Oscillographic display of the detected optical pulses*
a Input pulse
b Output pulse after propagation through 20 km long dispersion-free single-mode fibre at 1·5 μm
Horizontal scale = 500 ps/division